Chapter 16: Remote-Sensing Maps

MODERN GEOLOGICAL mapping is increasingly supported by a range of high-quality images of the ground surface obtained by various remote sensing devices. Such images give a bird's-eye view of the terrain, are used to map the principal geological features, and are indispensable for planning traverses on the ground. Enlargements may serve as base maps for plotting field data collected on the ground. Remote sensing has evolved into a major discipline within the earth sciences and should be studied in one or more course(s) dedicated exclusively to the subject. This chapter serves as a primer only and outlines some major principles and uses of images obtained by remote-sensing methods. Complementary and fuller coverage of the subject is found in specialist sources, cited in *Appendix A*. Sources of satellite images and aerial photographs are included in the *Additional Resources*.

Contents: The electromagnetic spectrum and its fundamental role in remote sensing are explained in section 16-1. Various platforms for recording electromagnetic radiation are outlined in section 16-2. Principles of aerial photography are discussed in section 16-3. Some methods of photo interpretation are introduced in section 16-4. Several satellite imaging systems, including Landsat and SPOT, are presented in sections 16-5 and 16-6. Digital image processing is briefly introduced in section 16-7. Examples of radar application are provided in section 16-8.

16-1 Electromagnetic spectrum

Taken literally, remote sensing is the observation of an object from a distance without touching the object. In geoscience, remote sensing is restricted to visualization of electromagnetic waves reflected and radiated from the ground surface. Gravity, magnetic, and electrical field geophysical surveys are beyond the scope of remote sensing as commonly used. Of course, such geophysical data are important for interpreting regional geological subsurface features. However, our attention concentrates on electromagnetic radiation patterns, recorded by a range of remote-sensing methods.

The electromagnetic spectrum consists of a continuum of energy traveling at the speed of light, 300,000 kilometers per second. It can be divided into several spectral bands, covering a particular range of wavelengths. Remote sensing refers to the spectral bands in terms of wavelengths, whereas electronic engineers communicate in terms of frequency bands. The relationship between wavelength bands (λ) and frequency (f) is given by the expression:

$$\lambda = c/f \qquad (16\text{-}1)$$

where c is the velocity of light. Obviously, shorter wavelengths have higher frequencies, and longer wavelengths have lower frequencies.

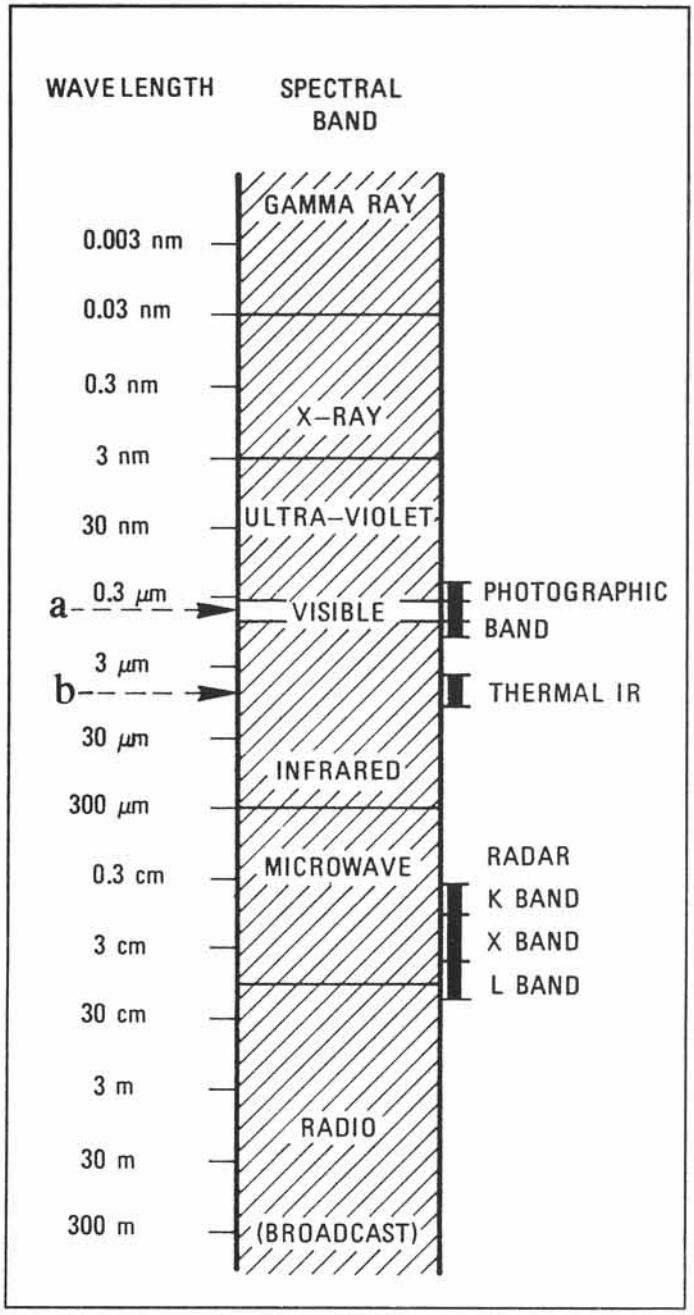

Figure 16-1: *Spectral bands of electromagnetic radiation, their corresponding wavelength range, and parts of the spectrum used in remote sensing.*

Figure 16-1 summarizes the major spectral bands of the electromagnetic spectrum used in remote sensing. The photographic band is seen to include light visible to the human eye plus parts of the ultraviolet and reflective infrared spectral bands. The thermal band covers thermal infrared wavelengths. Several radar bands (K, X, and L) are included in the microwave region of the electromagnetic spectrum. Radar is an *active remote sensing system*, transmitting microwave energy to the Earth's surface. The energy interacts with the terrain and is then returned to radar receivers aboard the airplane or spacecraft. In contrast, *passive imaging systems* utilize natural energy from the photographic and thermal infrared bands. These spectral bands receive natural radiation from the Earth's surface. The maximum intensity of natural electromagnetic energy occurs at 0.5μm for reflected (sun) light (arrow a, Fig. 16-1) and at 9.7 μm for thermal infrared energy, radiated at night and during the day (arrow b, Fig. 16-1).

☐Exercise 16-1: Photons may be considered physical particles, involved in the energy transfer of electromagnetic waves, traveling with the speed of light. Calculate the frequency ranges of cycles per second (or Hertz) involved in remote sensing of: (a) visible light (0.4 to 0.7 μm), (b) thermal infrared waves (1.3 to 14 μm), and (c) radarwaves (K-, X-, and L-bands between 0.8 and 30 cm).

16-2 Data collection

Photographs from the Earth's surface have been gathered since about 1850, using a range of vehicles: balloons, kites, pigeons, aircraft, rockets, and space probes. Classical aerial photography records images of electromagnetic radiation by means of chemicals on film. It was first widely used in aerial surveys for military intelligence operations during the First World War. Most aerial surveys detect visible light only, the most common form of electromagnetic energy, occupying wavelengths between 0.4 and 0.7μm. But portions of the adjacent UV-band (0.3 to 0.4 μm) and reflective IR-bands (0.7 to 0.9 μm) can, also, be utilized in conventional photography, provided that special film and filters are used.

Starting in the 1960's, technological advances of electromagnetic sensors, radio transmission, and computer technology allowed the color visualization of wavelength patterns in images of spectral bands other than that of visible light only. The data are commonly recorded in digital format, and an array of image-processing techniques allows visualization and enhancement of particular patterns in the monitored wavelength. Stored in a computer, they can be retrieved and processed at space imagery rectification centers into a wide variety of maps and images. The resulting images utilize gray scales and true or false colors to highlight contrasts in the recorded electromagnetic radiation.

Among the most common forms of modern satellite imaging data available to the general public are: Landsat, SPOT, Metric Camera, Large Format Camera, and KFA-100. Table 16-1 compares their scales of resolution and area coverage with that of conventional, low-altitude photographs. The resolution is the minimum length scale required for an object on the ground to become visible. The resolution of conventional photographs is still up to a hundred times better than that of any digital satellite image. More specifically, the most expensive techniques (Landsat and SPOT) have only moderate resolution (12 to 79 m). Nonetheless, the electronically enhanced Landsat and SPOT images are versatile and commonly yield geological information not visible on aerial photographs. One major advantage of Landsat images is that areas of 185 by 185 km are covered by a single image, allowing a synoptic overview of the region. Typical conventional aerial photographs cover only about 7 by 7 km each, so that many pictures are required to cover larger regions, and, thereby, major tectonic features may not be noticed.

Table 16-1: Altitude, frame size, and image resolution of some remote sensing platforms.

Platform	Technique	Oper.	Height (km)	Width (km)	Resol (m)
Landsat	multispectral	USA	920	185x185	80
	thematic mapper	USA	920	185x185	30
SPOT	multispectral	Fr	822	60x60	20
	panchromatic	Fr	822	60x60	10
Spacelab	Metric Camera	Ger	250	190x190	20
	Large Fm Cam	USA	250	700x700	8
	KFA-100	Russ	250	75x75	5
Airplane	low altitude photography	many	4	7x7	.3

☐Exercise 16-2: a) Compare and discuss some of the benefits and limitations of both satellite images and aerial photographs for geological mapping purposes. b) Also, compare the limitations and advantages of mapping by remote-sensing methods alone, with those occurring when the geological mapping is done exclusively by observations on the ground by a field geologist.

☐Exercise 16-3: Several remote-sensing images have appeared in previous chapters. Prepare a list of these remote-sensing images and photographs and specify which type of imagery was used.

16-3 Aerial photography

Aerial photographs are used for making and updating topographic contour-maps, monitoring land use, and serving as base maps for geological mapping. The potential benefits of aerial photographic studies to geologists are considerable. The photos help them to trace the boundaries between major rock units, to locate major folds, faults, joint patterns, karst or sinkholes, and other geological features. The extent of any superficial cover and distribution of good exposures of the bedrock can be quickly assessed. The accessibility of the terrain and proximity of interesting ground locations to roads and river beds can, also, be examined to prepare a detailed plan for an effective ground survey.

For any area of interest, there may be photographs available at different resolutions and scales, for different years and seasons, and from pictures taken with a variety of cameras and films. Study, and if necessary order, aerial photographs or satellite images (or both) of your prospective field area. Check what is available and what is best suited for your particular application. Before going into the field, prepare a photo-interpretation map and summarize your conclusions in a concise, written report. Aerial photographs are commonly available from various government and private agencies (see *Additional Resources*).

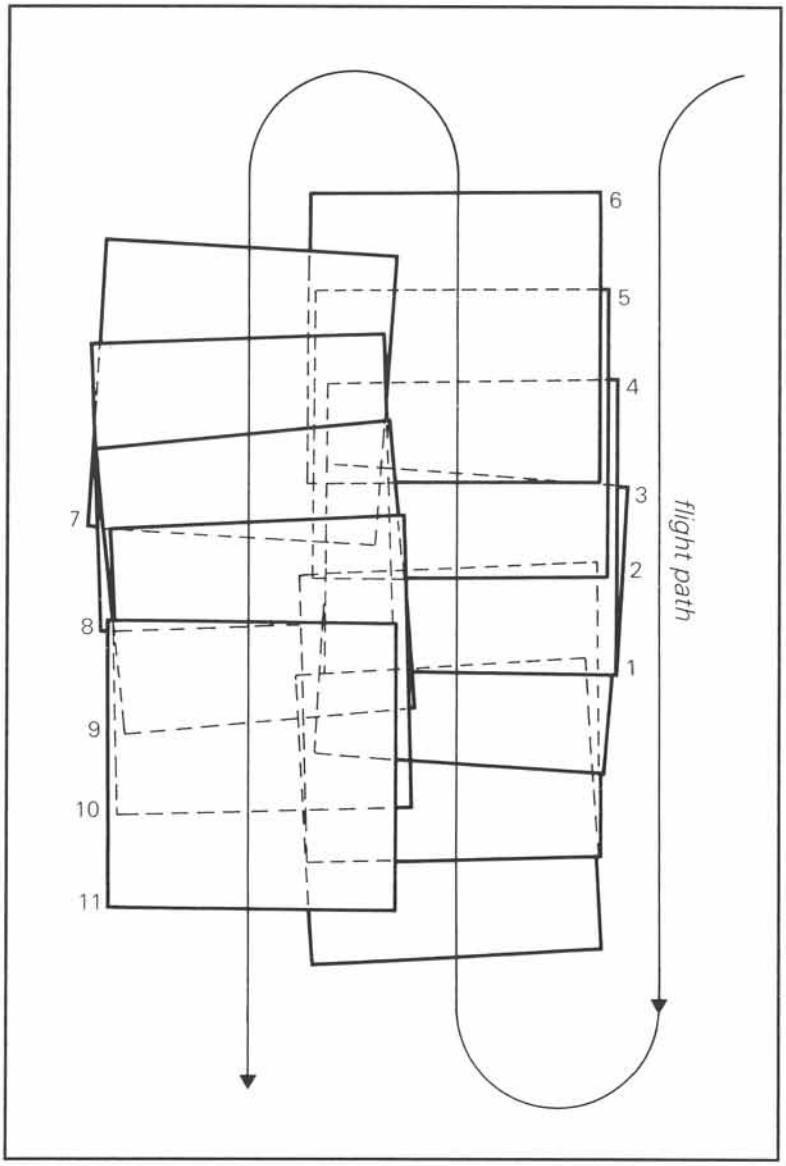

Figure 16-2: *The arrangement of individual photographs in an aerial survey is determined by the flight path of the aircraft.*

The resolving power of photographic film is exceptionally good compared to other forms of remote sensing (Table 16-1). Table 16-2 summarizes the minimum ground separation ($R_g/2$) on airphotos for a range of flight altitudes. The ground resolution (R_g) is obviously influenced by the system resolution, which resides in the quality of the camera and film. Table 16-2 uses two examples with resolutions of 40 line-pairs per mm and 100 line-pairs per mm, respectively. Table 16-3 lists the minimum ground separation required to recognize particular features. Rivers, urbanized and cultivated areas, and roadways can be easily recognized on aerial photographs. Likewise, a range of geological boundaries may be distinguished, based upon geological experience and expertise (section 16-4).

Table 16-2: *Ground separation limit on classical aerial photographs, for various standard scales.*

Altitude (m)	Scale	Ground separation for line pairs/mm 40 (m)	100 (m)
6,100	1:40,000	0.5	0.2
4,575	1:30,000	0.37	0.15
3,050	1:20,000	0.25	0.1
1,525	1:10,000	0.12	0.05

Table 16-3: *Features identifiable on aerial photographs of various ground separation limits.*

Ground separation (m)	Features identifiable
15	Rivers, mountains, and lakes
4.5	Cultivation parcels
1.5	Roads
0.15	Automobiles
0.05	Individual trees and people counts

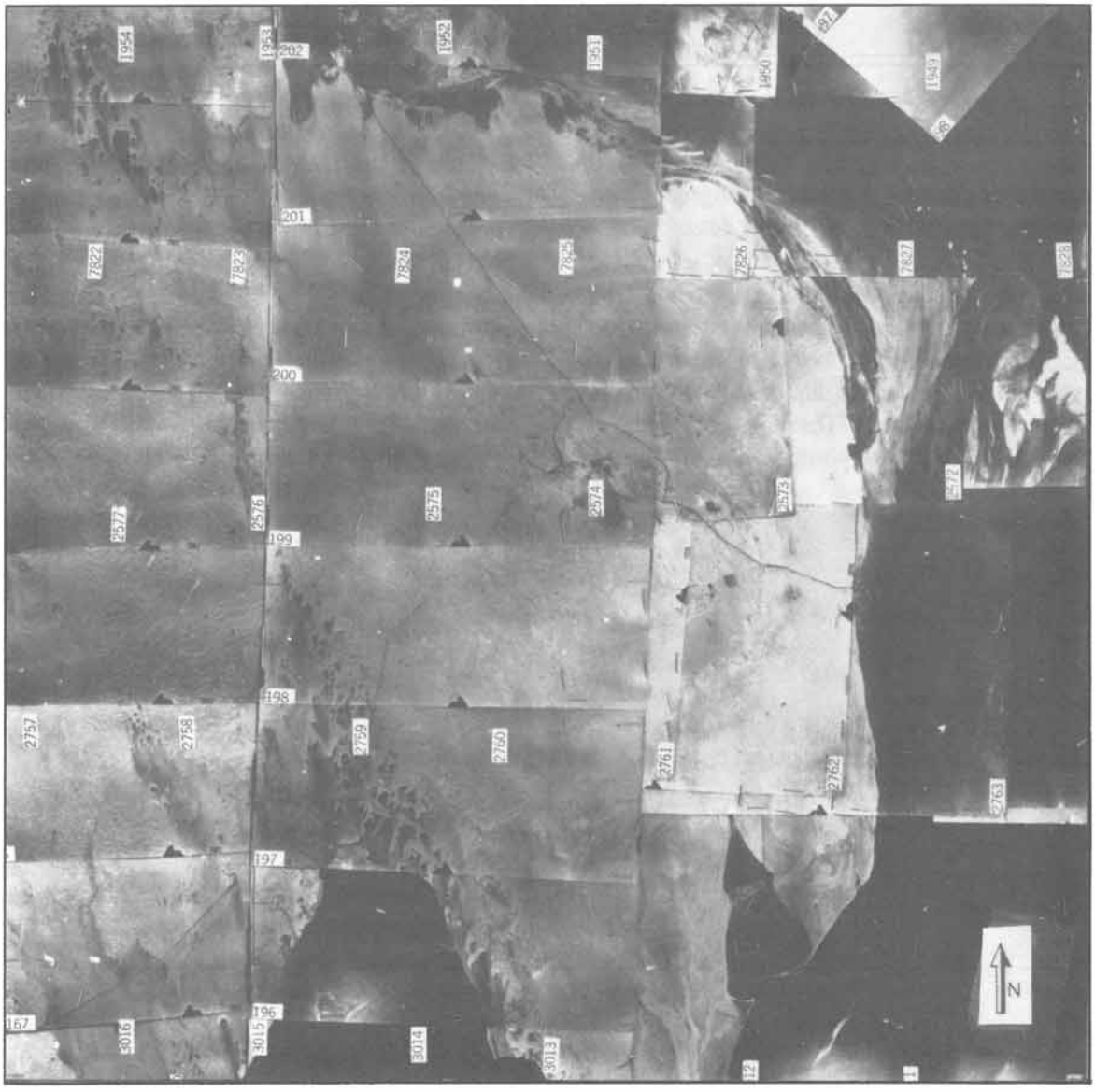

Figure 16-3: *Mosaic of high altitude aerial photographs of Dammam Dome at the Arabian Gulf, Saudi Arabia. This area shown in photomosaic is about thirty kilometers in width.*

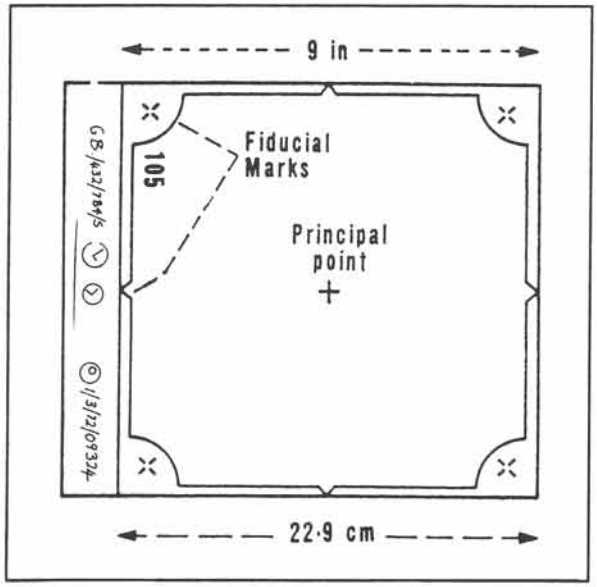

Figure 16-4: *Standard aerial photograph with fiducial marks (crosses) and flight data.*

Aerial photographs are commonly made from aircraft that fly parallel flight-paths or runs (Fig. 16-2). The frames within each run are spaced to ensure mutual overlap of about 60 percent between successive frames. There is, also, some 10 percent sidelap with the photographs of adjacent runs. Because each photograph covers only a limited area, tens to hundreds of photos are commonly needed to cover the ground for a regional survey. In order to locate the relative position of the pictures, a coverage diagram or index map is usually available from the agency supplying the prints. A print laydown or photomosaic, where the images are laid down in their approximate geographic location with serial numbers visible, is, also, very practical to keep track of the relative position of aerial photographs (Fig. 16-3). Small deviations from the planned flight path, due to variations in wind speed and direction, as well as thermal airflows, result in misalignment and slight rotation of adjacent photographs.

Each photograph is marked with flight numbers, serial numbers, flying altitude of the plane, focal length of the camera lens, date of photography and country represented (Fig. 16-4). The center or principal point of each photograph may be found at the intersection of each connecting fiducial mark at the margins of the frame. Overlapping photographs may be used to simulate a stereoscopic view or model of the terrain. Two images with considerable overlap, a so-called

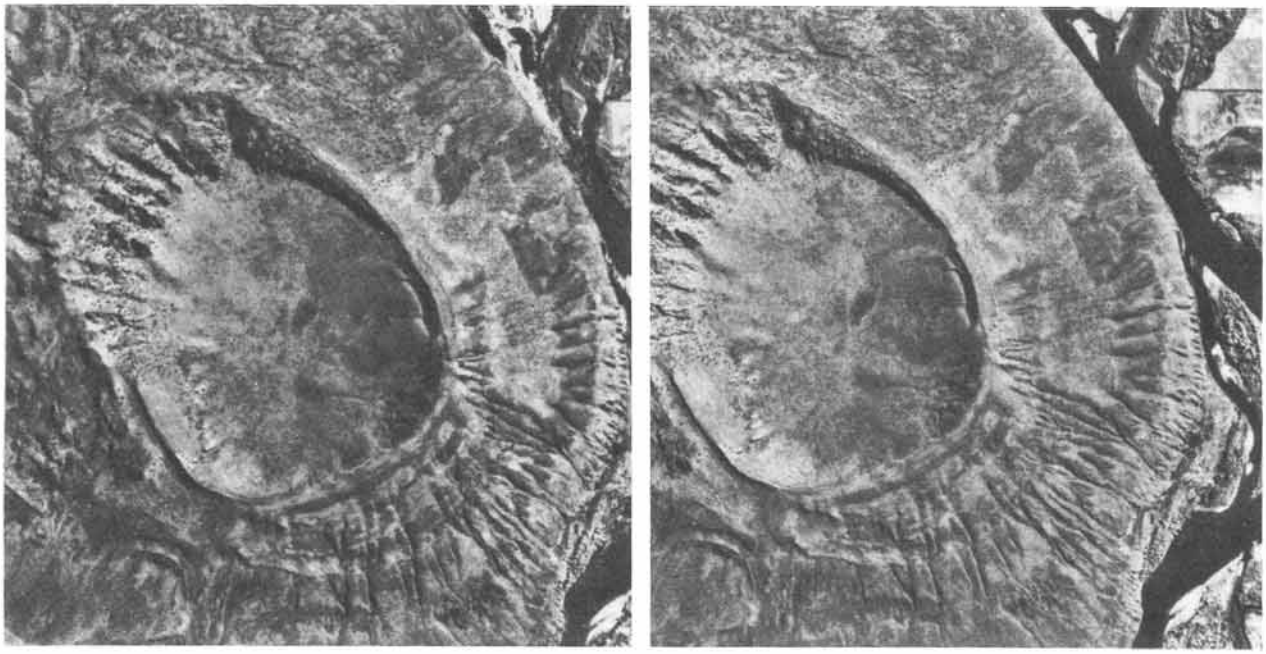

Figure 16-5: *Stereopair of Menan Buttes volcano, Idaho, USA. Image width is about 1.5 km.*

Figure 16-6a: *Stereoscope is used to create virtual-reality images of landscape from a stereopair of aerial photographs.*

Figure 16-6b: *Geologists make interpretation maps of aerial photographs on transparent overlays.*

stereopair, are laid down in a horizontal row. Only overlapping areas can create stereo vision, and it is important that these areas are similarly oriented with eye-base parallel to the flight line in each of the stereopairs studied. Figure 16-5 is a stereopair (showing only the cropped and overlapping portions of two adjacent aerial photographs) of the Menan Buttes volcano in southern Idaho, USA. The frame is 1.5 kilometers wide.

The illusion of a three-dimensional model of the landscape is created using a stereoscope (Fig. 16-6a). This is an optical device of various design, which aids the left and right eyes to merge the images of the left and right photographs into one stereoscopic view. The brain produces a three-dimensional view of the landscape, as seen directly from above at the time of the flight. Generally, there is a vertical exaggeration of two to four times the horizontal scale, which greatly aids geological interpretation and dip-strike estimation. With a little practice, and after adjusting the lens separation and photo positions, stereoscopic viewing becomes a powerful tool to examine the terrain in a bird's-eye view.

☐Exercise 16-4: A standard size of aerial photographic prints measures 22.9 by 22.9 cm (9 by 9 inches). Consider three common scales used, 1:60,000, 1:40,000, and 1:30,000, and calculate for each scale the dimensions of the corresponding ground area.

16-4 Photo interpretation

The aerial photograph reduces the ground surface to a scale that can be managed and analyzed in desk studies. A careful photogeology study closely examines the vast amount of data recorded on the images. The image shows variations in tone, texture, relief, size, and shape, as well as an inventory of the spatial distribution of surface features. The viewpoint provided in aerial images is unique and complementary to ground-based observations.

The study of aerial photographs can be done either with or without the use of stereopairs.

Experienced users may find they can do well without stereo enhancement, and the interpretation is done directly onto a single photograph. The very fine grain and large format film used in aerial photography sustain enlargements, if so required, without any significant quality loss. Even photostat copies and enlargements of good quality originals may provide useful bases for photo interpretations. The actual interpretations are traditionally done onto overlays of transparent tracing paper (Fig. 16-6b). Alternatively, analog aerial photographs can be scanned into digital format and interpretations can be traced on the computer screen, if so required. A relatively new trend in aerial photography is to use digital, rather than analog, cameras, so that advanced image processing is possible after acquiring the digital image files without need for scanning.

The information on aerial photographs is usually recorded in gray tones of the black and white scale. The photograph records the light reflected by the ground surface. The ratio of reflected energy to incident energy is called the albedo. Dark surfaces have low albedos, and light surfaces have high albedos. The tone of the image is affected, not only by the nature of the surface photographed, but also by such factors as atmospheric conditions, solar position, film properties, flight schedule, and camera performance.

Figure 16-7: *Oblique aerial view of inclined sedimentary beds. Dip is to the left. Road for scale.*

The photographic appearance of the terrain is, also, affected by vegetation, drainage patterns, soil cover, jointing, weathering, erosion rates, rock composition, deformation structures, and other geological features, such as karsting, bedding and volcanism. Another feature affecting photo interpretation is the topographic relief of the terrain. It should be kept in mind that all slopes of both bedding and any topographic relief often appear much steeper in the stereoview than in reality. However, vertical exaggeration is usually a desirable artifact of the stereoscopic set-up. The direction of dip of layers can be inferred from the V-shaped intersection, where geological boundaries are cut by major valleys. Generally, the V-pattern points down-dip where beds cross stream-channels. Figure 16-7 is an oblique aerial photograph of uniformly dipping sedimentary strata with a geomorphology defined by linear ridges and flat-irons of dip-slopes, transected by a parallel drainage pattern. Patterns of drainage networks can take on many distinct forms, often related to the underlying geology. A regional plateau, made up of horizontal strata, may be transected by meandering rivers (Fig. 16-8). Other basic drainage patterns are illustrated in

Figure 16-9a to f. Many more variations and combinations of drainage patterns are found in nature, but nearly all may be related to the basic patterns shown.

In spite of the variability in tone, comparison of the relative tonal values within an image may help to distinguish rock units. Rocks composed of mafic minerals tend to absorb much radiation and appear with dark tones on the image (gabbros, basalts, and amphibolites). Rocks of felsic minerals and evaporites tend to appear as light tones on the image (granites, sandstones, and carbonates). Intermediate tones are produced by diorites, shales, slates, and schists. Water in rivers, lakes, and seas absorbs radiation and, therefore, has a dark tone on aerial photographs. In addition to tone and texture, shape and size may help to differentiate further between rock units. For example, intrusive bodies of granite, diorite, and gabbro are all likely to be subcircular with diameters ranging between one to ten kilometers. Intrusive bodies are typically transected by joint patterns, which commonly control the drainage network into rectangular and trellis patterns. Sedimentary rocks are typically layered and include boundaries with sharp tonal contrasts. Carbonates may be distinguished from sandstone units by the presence of sinkholes. Metamorphic rocks are typically foliated but have fewer sharp tonal or color contrasts, due to the homogenizing effect of mineralogical changes induced by metamorphism.

A photogeological interpretation can progress systematically, following the hints given below: (1) Assess the nature and extent of vegetation, together with the climatic environment (humid, arid, temperate, or tropical). (2) Describe the topography of the terrain, geomorphology, and

Figure 16-8: *Low-altitude, oblique aerial photograph of a terrain made up of horizontally bedded sedimentary rocks, transected by a meandering river, USA.*

type of drainage pattern. (3) Mention any major culture and settlement centers. (4) Decide what erosional agent is dominant in the area studied (wind, ice, water). Before proceeding, use a transparent overlay on top of the photograph to draw a geological interpretation map. Start your map by drawing a frame around the area, include a scale bar and north arrow, and mark the map with photo fiducial marks and serial numbers, together with a suitable name for the area studied. Then proceed as follows: (5) Divide the region into areas covered by surfical deposits, and outline the major exposures. (6) Establish the nature of the bedrock (sedimentary, metamorphic, or igneous rocks). (7) Trace the boundaries between the major rock units. (8) Include structural symbols on the map for strike and dip of strata, mark traces of faults and fold axes, indicate antiforms, synforms, and sense of movement on faults. Common symbols used on the interpretation maps of remote-sensing images are given in Figure 16-10. (9) Include a legend with your photo-interpretation map. (10) Consider the geological history of the area. (11) Write an outline to accompany your map, addressing the topics and features mentioned under points 1 to 10.

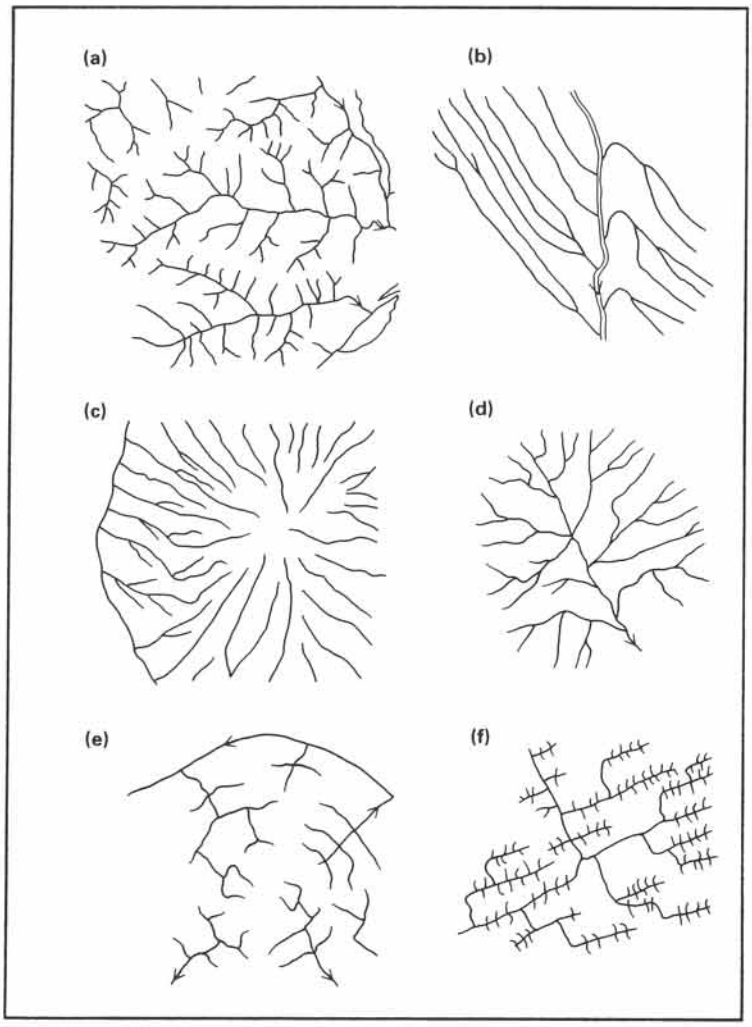

Figure 16-9: *Basic forms of drainage patterns: (a) dendritic, (b) parallel, (c) radial, (d) centripetal, (e) annular, and (f) trellis.*

Some examples of aerial photographs of different terrains are shown in Figures 16-11 to 16-14. Figure 16-11 is a stereopair of vertical aerial photographs showing *barchan dunes* in the Californian Mojave Desert. Figure 16-12 is a stereopair of vertical airphotos of folded strata in Wyoming, USA. Figure 16-13 is a stereopair of the Precambrian shield of western Saudi Arabia. The area comprises granitic intrusions and foliated supracrustals (schists), transected by basic dikes and fault off-sets. Figure 16-14 is a stereopair of Tertiary flood basalt, erupted onto eroded Precambrian basement of the Arabian shield. Visible are basic feeder dikes, transecting jointed plutons and foliated supracrustals of the basement.

☐Exercise 16-5: Make photo-geologic interpretation maps of the areas in Figure 16-11 to 16-14. Accompany each map with a written outline, discussing the items of points 1 to 10, mentioned in section 16-4.

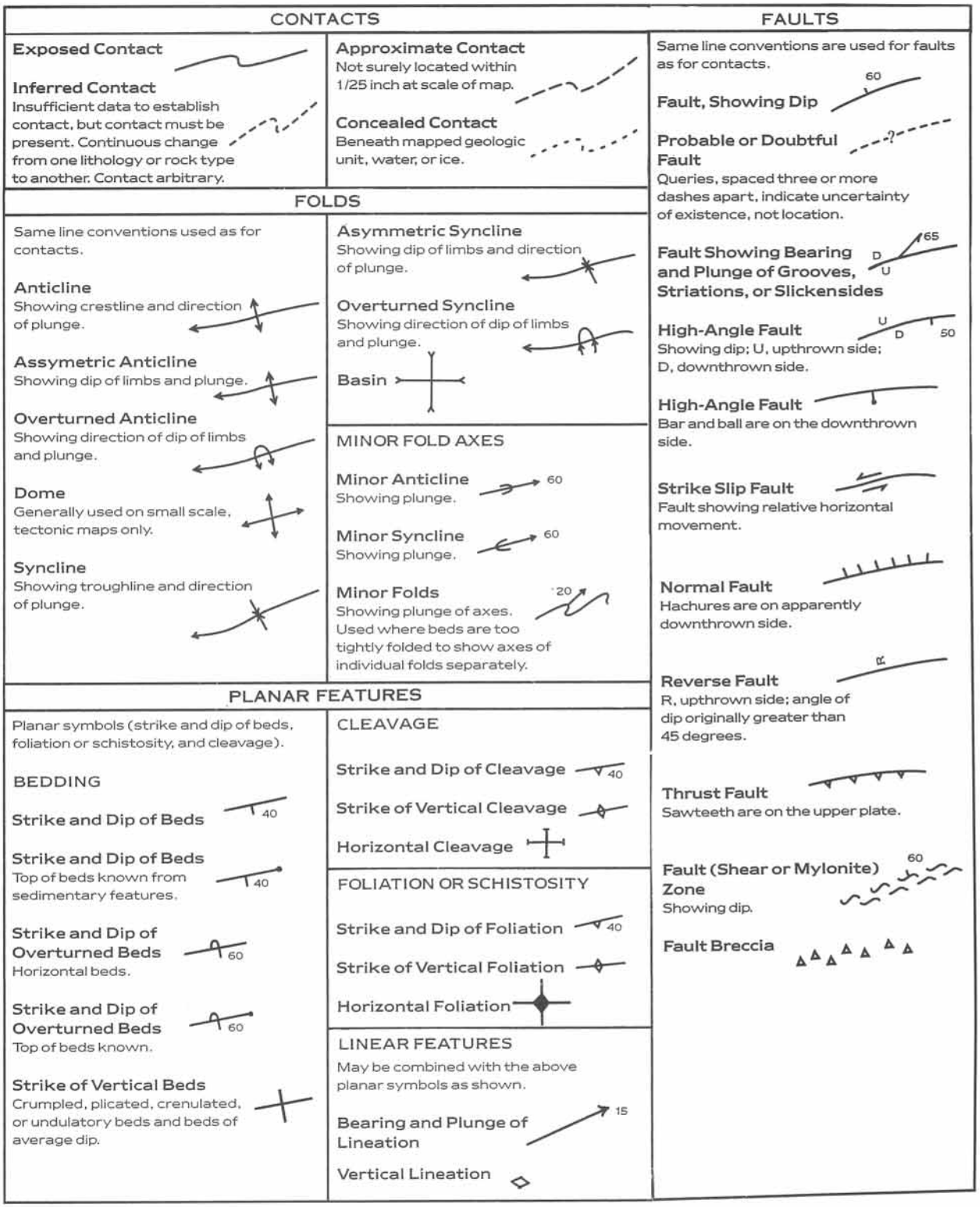

Figure 16-10: *Symbols suitable for use on photo interpretation maps. However, symbols are not standardized, and many different symbols are in use throughout the world.*

Figure 16-11: *Stereopair of sand dunes, Mojave Desert, California. Image width is about 1.5 kilometers.*

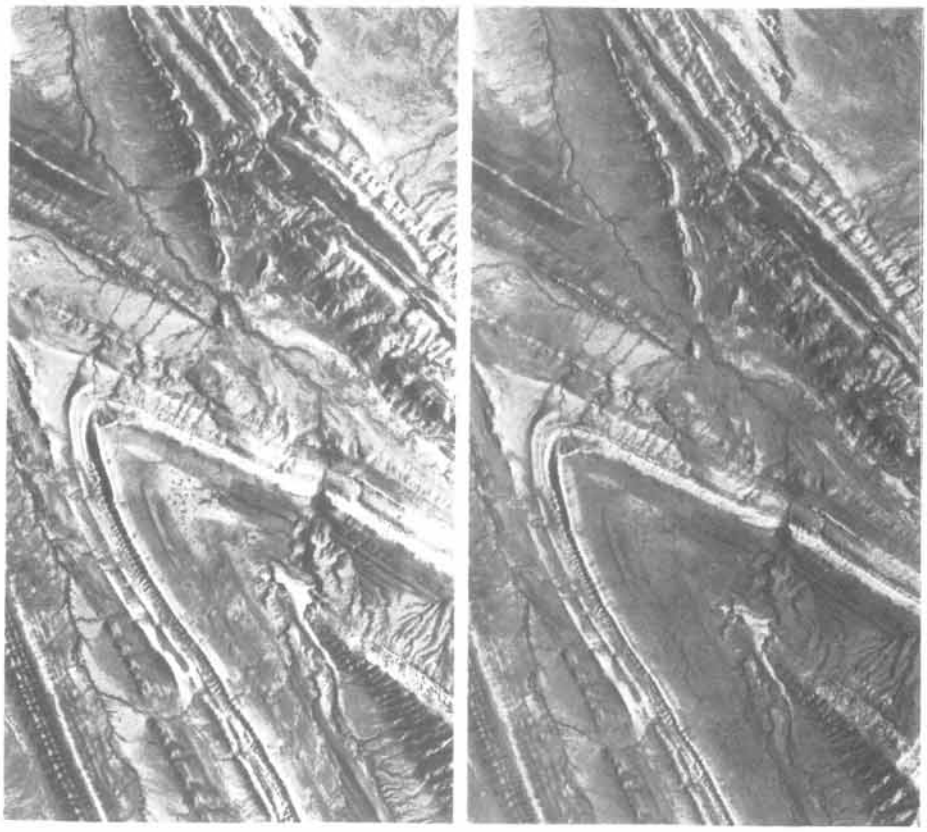

Figure 16-12: *Folded sequence. Image width is about two kilometers.*

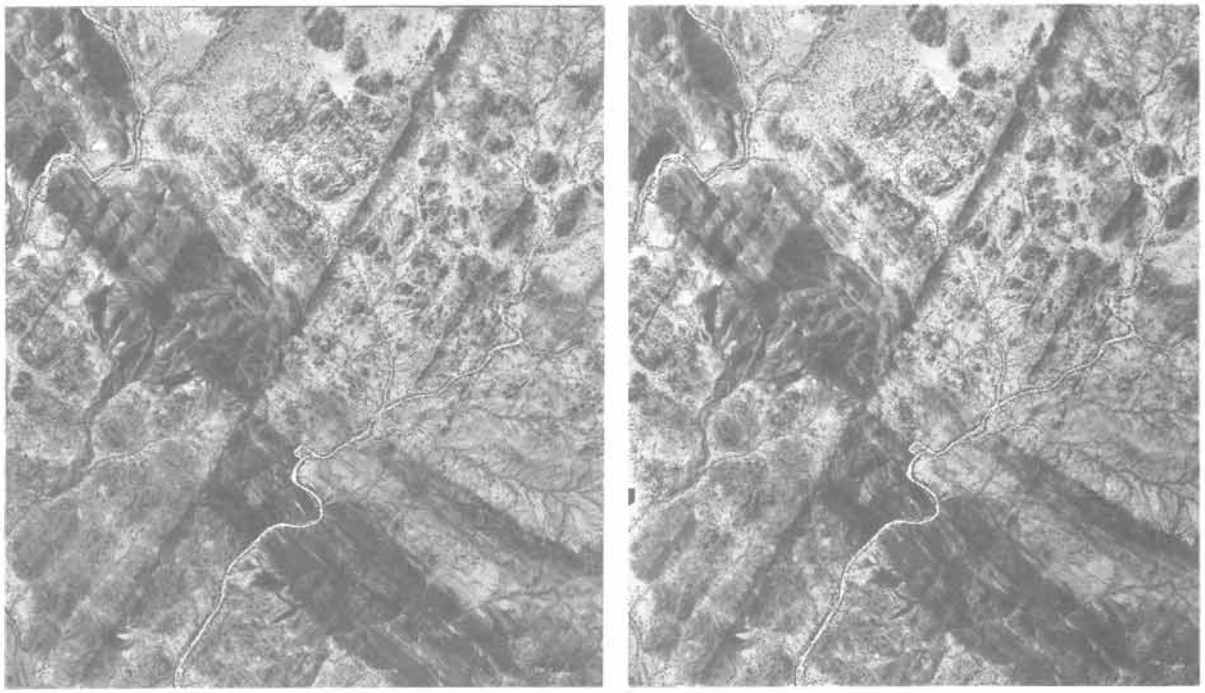

Figure 16-13: *Stereopair of fractured supracrustals and igneous basement. Basic dikes intrude the fractures parallel to the fault. Image width is about four kilometers.*

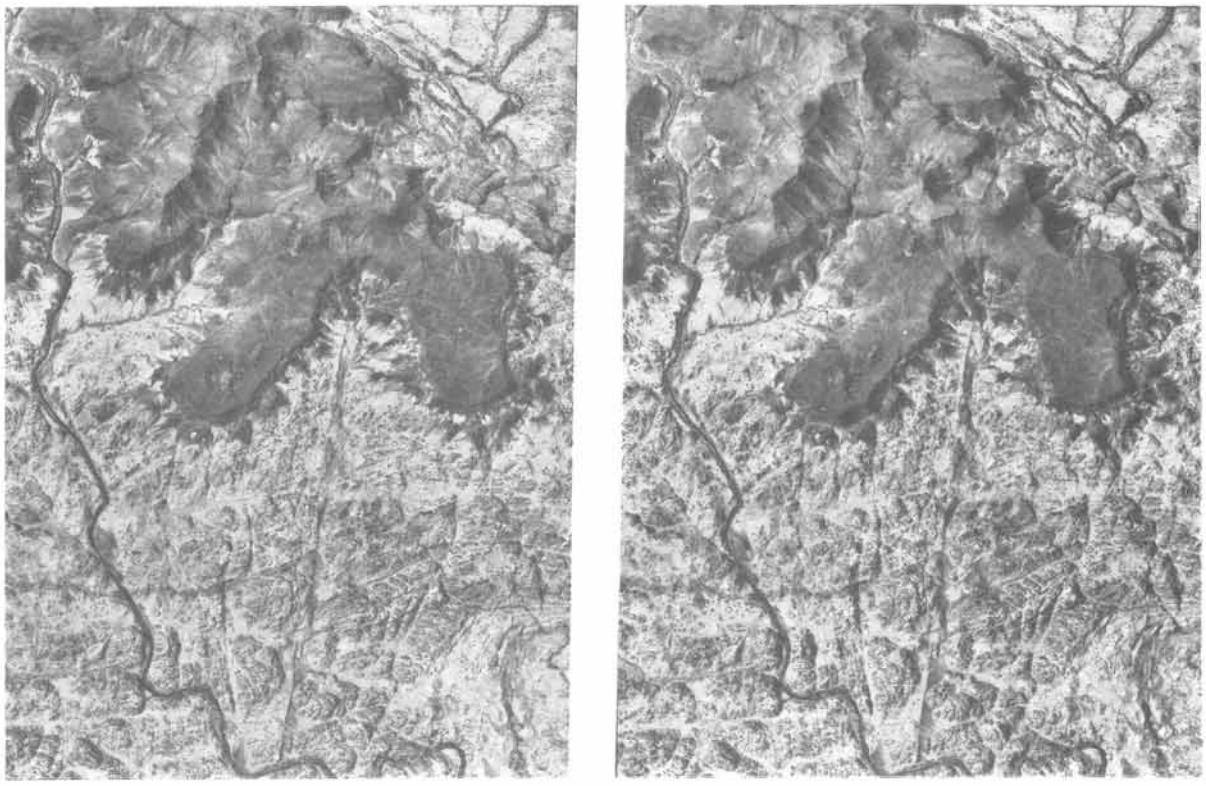

Figure 16-14: *Stereopair of Tertiary plateau basalt, resting on Precambrian basement rocks of the Arabian shield. Image width is about 2.5 kilometers.*

16-5 Satellite images

Satellite images have a number of advantages over classical aerial photographs. They cover much larger areas, they allow coverage of areas with inaccessible air space, and they are routinely collected and updated by space agencies and, therefore, can be ordered on demand without loss of time. Radial distortion, a problem when making maps from airphotos, is not present on Landsat and SPOT images. Modern satellite images are recorded digitally. Consequently, they can be processed with the aid of sophisticated software to enhance particular features in the image by introducing color coding, and by the shifting and filtering of wavelengths.

Table 16-4: Selection of satellite based remote sensing imagery systems.

Satellite	Scene size (km)	Resolution (m)	Bands
Landsat MSS	185x185	79	four
Landsat TMS	185x185	30	seven
SPOT	60x60	20-10	four
	Swath width (km)	**Resolution (m)**	**Bands**
Tiros	2,100	1,100	five
Nimbus	1,600	825	six
HCMM	715	600	two
Seasat	100	25	one

More recently, satellite imagery is promoting a technology called Quantitative Structural Mapping (QSM). The idea is to create maps using data from satellites, rather than measurements on the ground, principally because detailed ground-based studies are costly and time-consuming. Obviously, one of the strengths of remote sensing is that it gives instantaneous access to any place in the world. No permission is required to enter the terrain, and cumbersome ground logistics are avoided. Digital elevation data from satellite probes can be merged with electromagnetic radiation data to produce detailed perspective views of a terrain (Fig. 16-15). In such images the terrain can be coded, such as to outline boundaries between rock units, faultlines, fold axes, and strike and dip of bedding. Remote sensing, thus, helps to determine the overall structural grain and major lithological subdivisions. Although being a powerful high-tech aid to mapping work, QSM is unlikely to replace geolo-

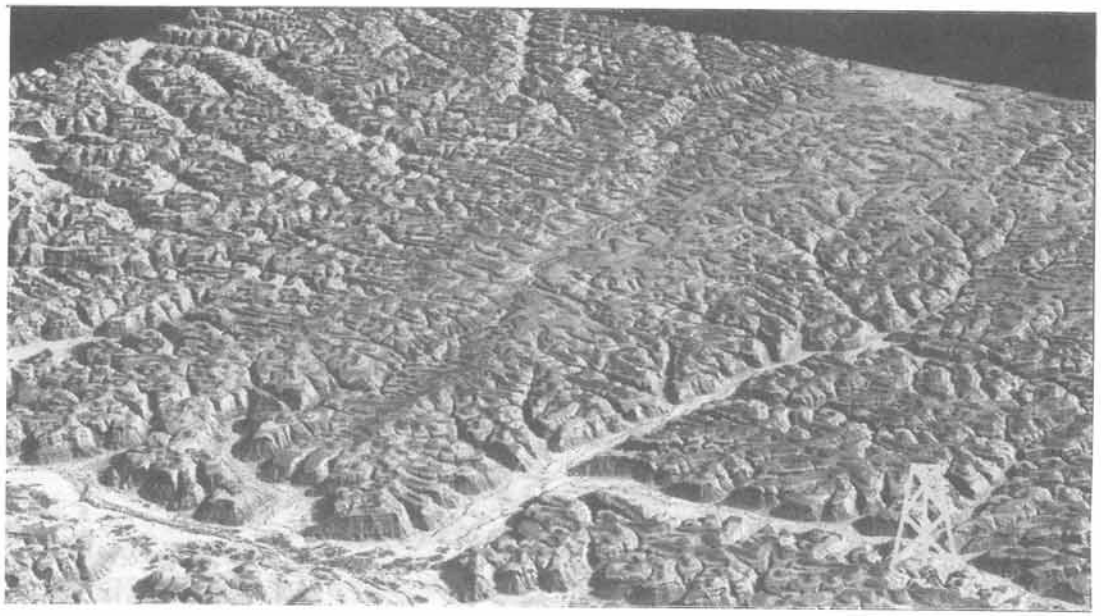

Figure 16-15: *Digital animation of landscape in Yemen. Surface geology can be included in the original image by projecting satellite imagery onto the land surface.*

gical field work altogether. But it has already been applied successfully in petroleum exploration programs of remote, arid regions.

Returning to our discussion of basic satellite imagery, many different satellites have been launched to collect electromagnetic radiation scans of the ground surface (Table 16-4). Some of these satellites were launched principally for monitoring oceanic currents, sea floor bathymetry, and weather patterns. Their images cover very large areas, but with low resolution. The resolution of some satellites is so low that no detailed geological observations can be made. For example, ground resolution of Tiros, Nimbus, and HCMM is 1,100, 825 and 600 meters, respectively. Seasat records microwaves of 23.5 cm wavelength and maps the bathymetry and tectonics of the sea floor by determining lateral changes of sea-level. However, it reveals little ground contrast, rendering it largely unsuitable for geological studies of continental areas.

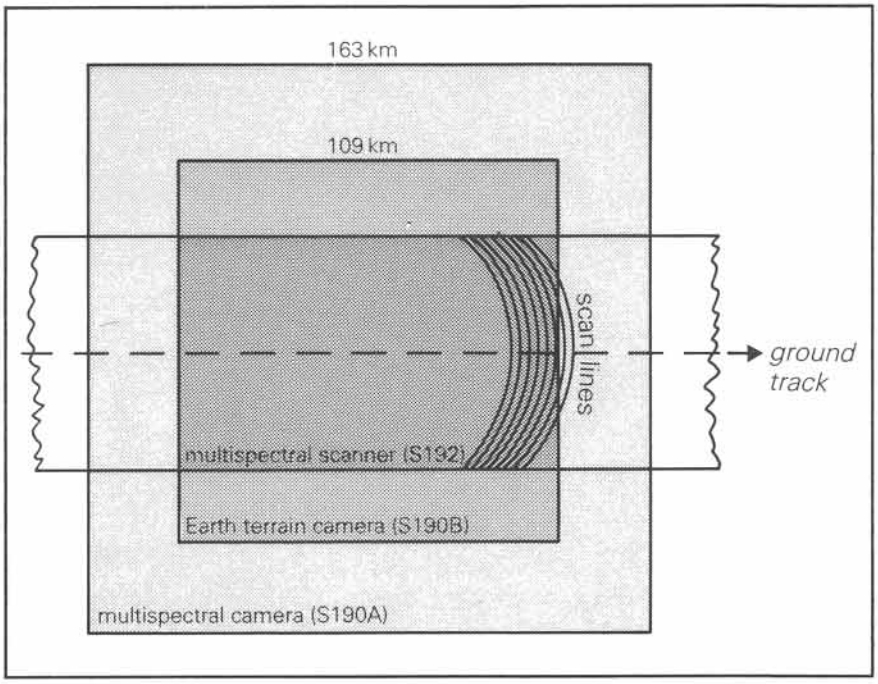

Figure 16-16: *Ground track, swath width, and movement of scan lines in different imaging devices.*

The Gemini and Apollo NASA missions of the 1960's included manned spacecraft, which collected satellite images of the Earth's surface with handheld cameras. But most modern, unmanned spacecraft collect images by electromagnetic sensors, mostly with line-scanning techniques. The forward motion of the Landsat spacecraft allows successive elements of the ground to be scanned by detectors of electromagnetic radiation (Fig. 16-16). The scanner is in a fixed position inside the spacecraft and receives electromagnetic radiation via a scan mirror, sweeping back and forth to cover a particular width of the terrain below. The mirror reflects the radiation onto arrays of detectors, transforming the radiation into a digital signal. The radiation collected by the sensors is usually filtered and differentiated into bands of the visible and infrared wavebands. The ground is covered in sweeps perpendicular to the flight motion and at a rate matching the ground speed, thus ensuring complete coverage of each swath.

☐Exercise 16-6: The United States can be covered completely by approximately five hundred Landsat images. a) Estimate how many SPOT images are required to cover the same area. b) How many conventional aerial photographs are required?

16-6 Landsat and SPOT images

The best ground resolution in satellite images, available to the public, is presently provided by Landsat thematic mapper and SPOT images. Various generations of Landsat spacecraft, the first of which was launched by NASA in 1972, have collected multispectral scanner images

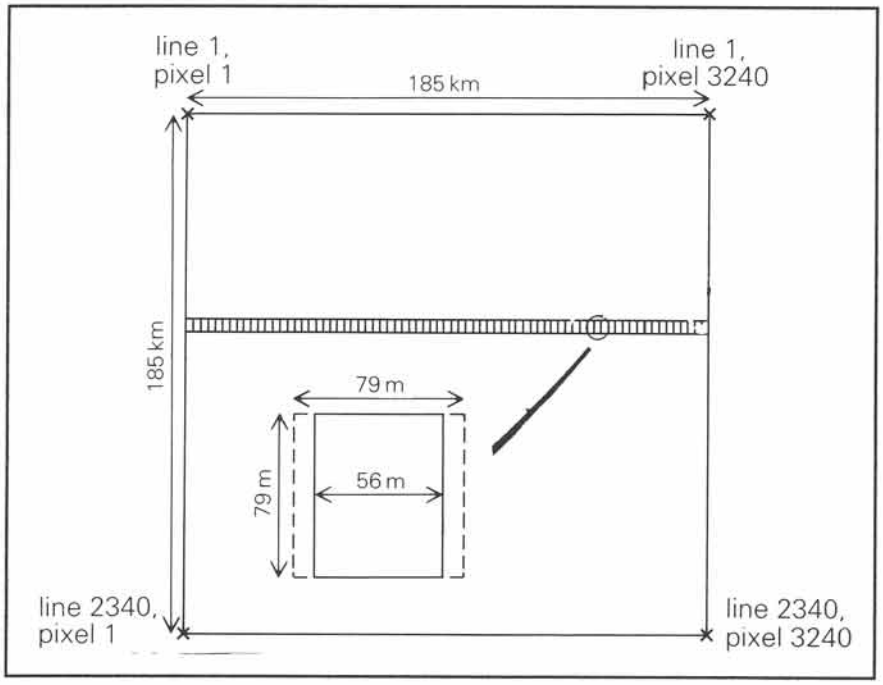

Figure 16-17: *Pixel arrangement and size in Landsat MSS images.*

(MSS) and, more recently, thematic mapper images (TM). Careful study of satellite images reveals that they are constituted by a pattern of regular lines and columns made up of pixels or picture elements. Each pixel displays either a gray tone or a particular color. For example, each MSS Landsat image is composed of 2340 scan lines, and each line is composed of 3240 pixels. The ground size of the pixel determines the maximum resolution of the image. For Landsat MSS images, each pixel represents the average wavelength intensity for a ground area of 79 by 56 meters (Fig. 16-17). Pixel size of Landsat TM images is 30 by 30 meters,

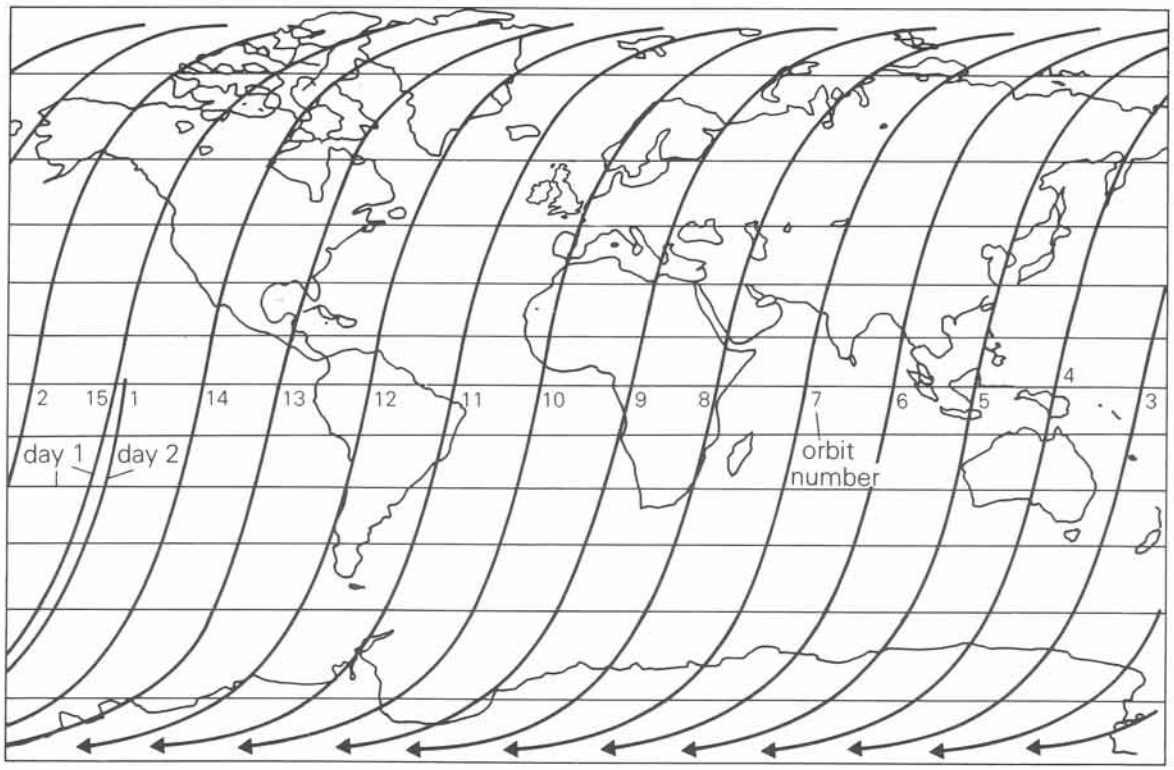

Figure 16-18: *Ground tracks of successive Landsat orbits with arbitrary flight path numbers. Orbits descend at day side, shown here, but ascend at night side of the Earth.*

while pixel size of SPOT is 12 by 12 meters for panchromatic and 20 by 20 meters for color images.

The area covered by satellite images is commonly limited by the width of the swath covered by the sensor array, either fixed or connected to a scan mirror sweeping back and forth. For Landsat, the standard image covers 185 by 185 kilometers. SPOT, which has a fixed array of electromagnetic sensors and no sweeping mirrors, covers a smaller ground area of 60 by 60 kilometers in each image. Landsat circles the Earth in near-polar orbits once every 103 minutes, between 800 and 900 kilometers altitude, and is sun-synchronous. All images, therefore, receive radiation from the visible electromagnetic spectrum, and nearly the same point on the ground is repeated every 18 days. Each orbital swath is 2,760 kilometers west of the immediate predecessor (Fig. 16-18). The groundtrack of the swaths do not closely follow meridians, but are oblique to them, because the Earth rotates away underneath the satellite, which follows a near-polar orbit. Incidentally, the name of the Landsat program was given as a complement to the Seasat program, as it was designed to obtain information from land rather than sea areas. However, Landsat was launched before Seasat and was initially called ERTS.

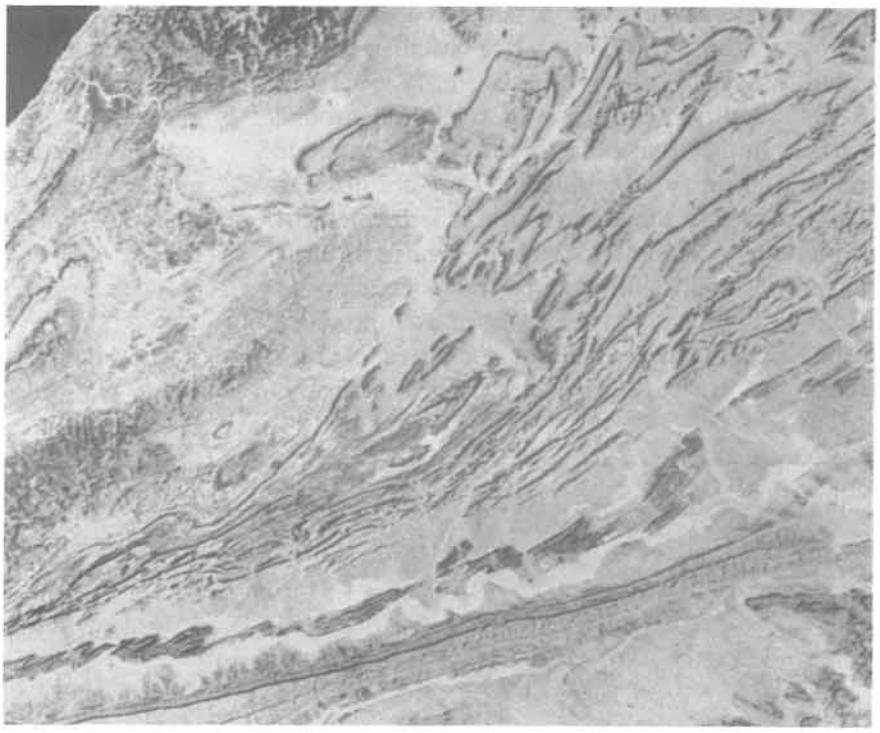

Figure 16-19a: *Part of Landsat MSS of dextral Moroccan Border fault, separating Tindouf basin of the Draa Plateau to the south from tightly folded Devonian limestone and sandstone in the north wall.*

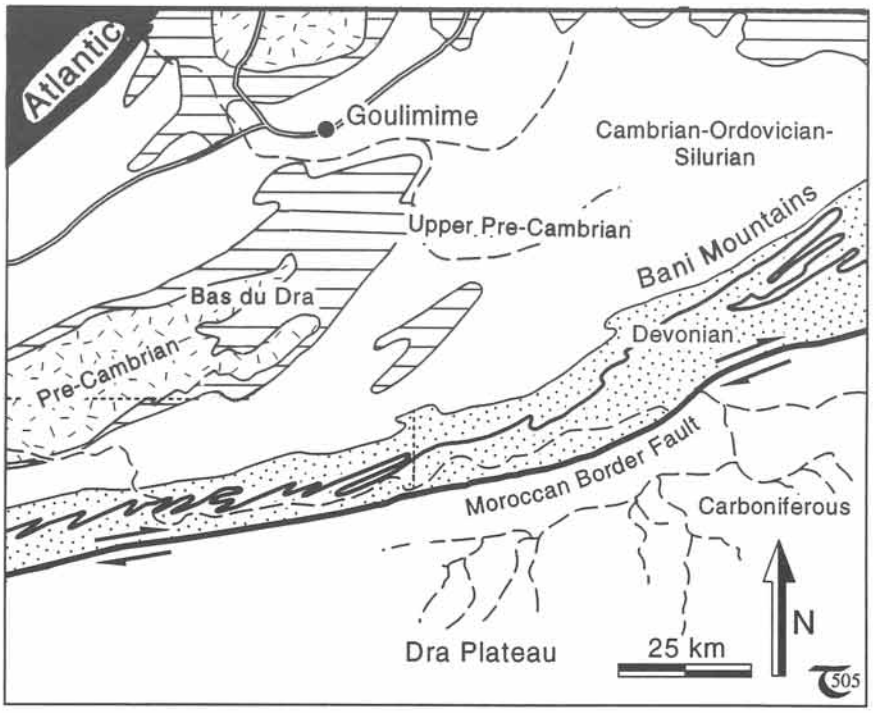

Figure 16-19b: *Interpretation map of Landsat image of Figure 16-6a. Precambrian basement inliers are ruled and shaded.*

SPOT, an acronym for Satellite Probatoir pour l'Observation de la Terre, is a Swedish-French satellite system, first launched in 1986. Three SPOT satellites concurrently track the ground surface in different polar orbits, completing one revolution every 101 minutes. They are orbiting 830 kilometers above the Earth and complete 14 orbits every 24 hours. Because the Earth turns under the satellite, the ground track of each orbit is 2,823 kilometers farther west of each previous orbit. SPOT images are not composed of line-scans but are measured directly by an array, consisting of thousands of micro-detectors or charge-coupled devices (CCD's). The radiation from the ground is directly measured without any mirroring, as the CCD-array moves with the spacecraft over the ground area. In multispectral mode, 3,000 CCD's sample the ground pixels, leading to a pixel size of 20 meters. Panchromatic images are built up from 6,000 CCD's and produce a pixel size of up to 12 meters.

The pixel resolution on SPOT images is still one to two orders of magnitude less than that of low altitude aerial photographs, but better than that of Landsat. Figure 16-19a is part of a composite image of southern Morocco, 150 km from E to W and 225 km from N to S, taken from 817 km altitude by the Landsat spacecraft on March 27, 1973. A geological interpretation is outlined in the map of Figure 16-19b. For comparison, a SPOT image of part of the region is shown in Figure 16-20. This arid region, with only 10 to 15 centimeters of annual precipitation, exposes a geological history from the Precambrian to the present. The semicircular Precambrian basement inlier of Sidi Ifni, near the Atlantic in the northwest (black), is covered by gently folded sedimentary rocks of Paleozoic age. In the south, the meandering Draa Valley

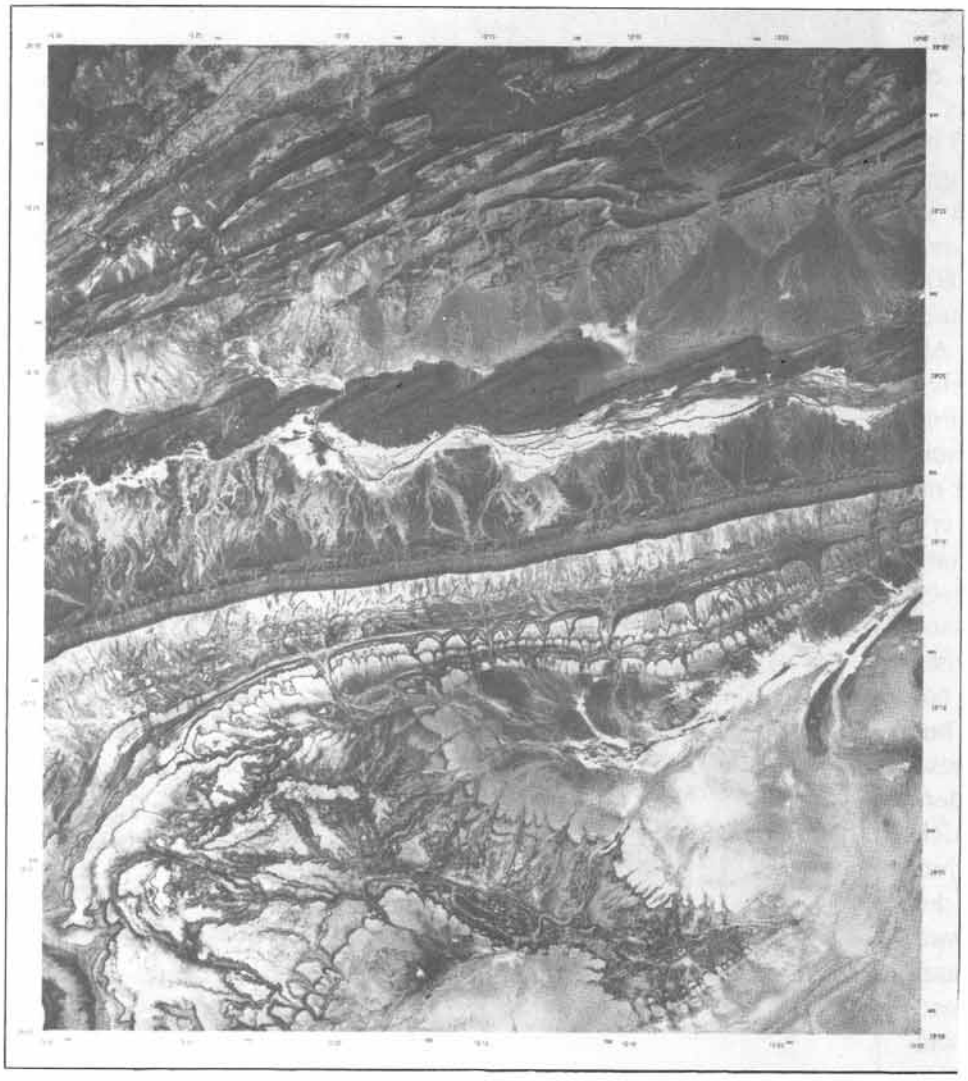

Figure 16-20: *SPOT image of Draa Plateau and Draa Valley, immediately south of the folded Devonian sequence. Image width is sixty kilometers. Compare pixel resolution with that of Figure 16-19a.*

(white) covers the dextral Moroccan Border fault, which separates the subhorizontal Carboniferous sequence of the Tindouf basin in the south wall from the tightly folded Devonian limestone and sandstone in the north wall. The dextral sense of displacement along the Moroccan Border fault is obvious from asymmetric folds in the Devonian sequence in the north side of the fault.

☐Exercise 16-7: Make a geological interpretation map for the area imaged in Figure 16-20. Accompany the map with a written outline, covering, also, the topics discussed in points 1 to 10 of section 16-4.

16-7 Basic image processing

One basic step in image acquisition is the assessment of the original ground data and translating this into pixel tone or color for each pixel. The analogue data from each electromagnetic detector are electronically filtered and calibrated. The quality of the final signal is dependent on the signal-to-noise ratio, which is controlled by: (1) the sensitivity of the detector for recording a particular wavelength, (2) the width of the waveband, (3) the intensity and range of radiation received from the ground surface, and (4) sensor altitude and spacecraft velocity. The scans are beamed down to a ground station in digital form, where they are corrected for distortions.

The actual image is obtained by modulating and rebuilding the scan into an image of pixels, which may be either in color or panchromatic (i.e., exclusively in gray tones). This is commonly achieved by scaling the energy of a waveband received by a detector for each pixel with a digital number (DN). Figure 16-21 shows an example of a histogram, showing the frequency or number of pixels that received energy, as expressed by DN's between 0 and 255 for computer compatability. DN-values of zero correspond to a minimum intensity for electromagnetic radiation wavelengths received (black on the image), and maximum values are scaled as 255 (white on the image). Intermediate brightness values are represented by intermediate DN's and gray shades on the image.

After scaling the basic radiation signal by DN's, image patterns can be described in strictly numerical terms by locating each pixel with an XY position on the image surface, together with a corresponding DN for tone or color value. An example of spatially arranged digital pixel values is illustrated in Figure 16-22a. The energy level of electromagnetic radiation represented by each pixel can be better visualized by assigning particular gray tones to a range of close DN-values. The corresponding computer print-out in gray-scale display is shown in Figure 16-22b. Similar-

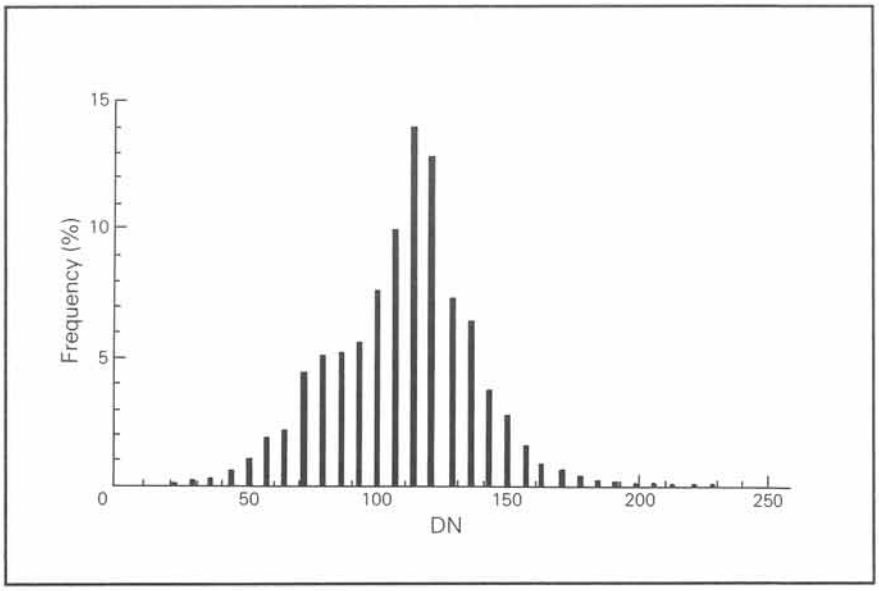

Figure 16-21: Number or frequency of pixels that received electromagnetic energy of the level indicated by a Digital Number (DN), scaled from 0 to 255.

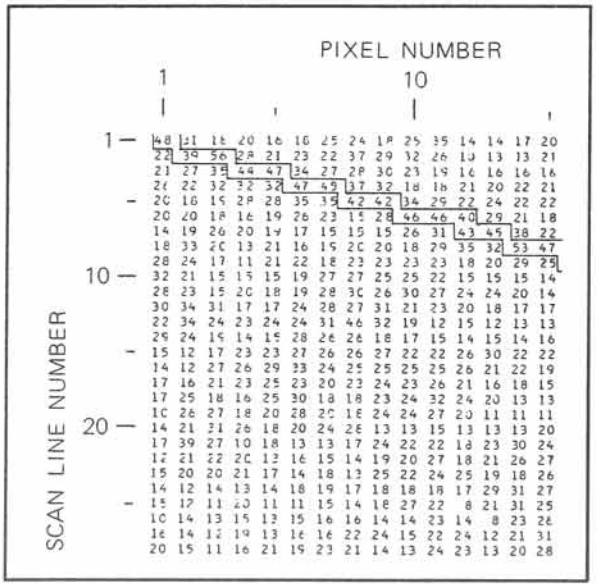

Figure 16-22a: Spatial arrangement of pixels and their DN values in digital image.

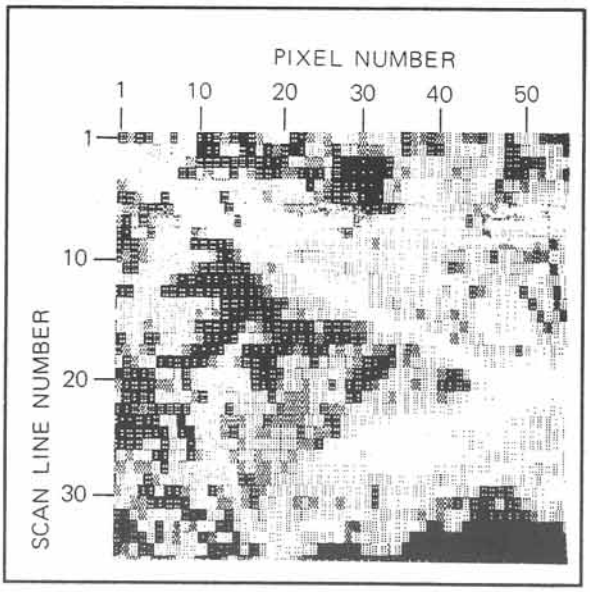

Figure 16-22b: Pixels of digital image, scaled by gray scale display.

ly, a color display could be generated by assigning particular colors, rather than gray tones, to each DN or to a group of DN's. If the colors are different from that of the original colors on the ground such an image is called a false or pseudo color image.

One type of image enhancement can be achieved by manipulating the digital data so that pixels with relatively small differences in DN are displayed with distinct contrast either of color or in gray tones (Fig. 16-23a & b). The density contrast stretching enhancement is principally achieved by reassigning a broader range of DN's to pixels receiving 92 percent of the radiation. In the example shown, an original DN of 49 is rebased to DN of zero, and an original DN of 106 is rescaled to 255. The intermediate values are stretched in between to enhance the contrast in DN's, and the resulting image shows much clearer contrast between ground features of different albedo. Other forms of image processing are aimed at restoring bad sectors due to malfunctioning of the electromagnetic radiation detectors. The image is restored by assigning DN's intermediate to neighboring pixels if original data are missing.

Processing methods can, also, concentrate on the visualization of the energy exclusively received within a particular band of wavelengths. But, if various types of detectors are used in the remote sensing platform, this allows for blending and separation of wavelength bands. The image can be redressed by ratioing bands. For example, the Landsat MSS system can provide each pixel with the energy levels of, at least, four wavelength ranges (Bands 4 for visible green light, 5 for visible red light, and 6 and 7 for parts of the reflective infrared spectrum). Landsat's TM detects seven bands within the electromagnetic spectrum: reflected blue, green, and red light, and four infrared bands. Particular bands favor rock contrast, while some combinations may obscure their distinction. For example, Figure 16-24a shows good bedrock contrast in an area of south India, using Landsat MSS band 7 only. Figure 16-24b displays the same area, using the band 7 and band 5 ratios. This brings out the spectral properties of vegetation but obscures the radiation of underlying bedrock units. Processed images may show rock types in different, false colors, although the original scanner does not necessarily measure any true colors.

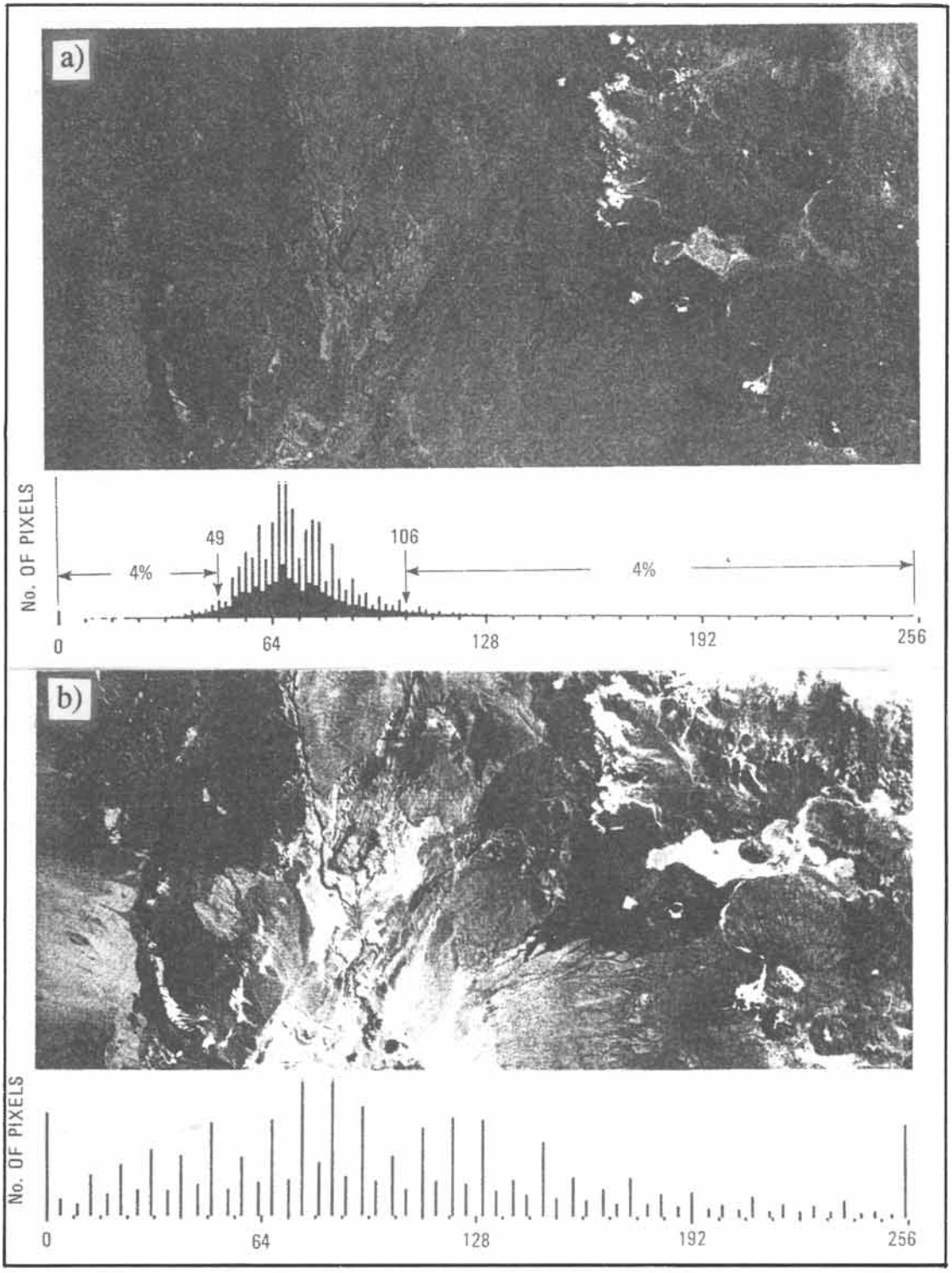

Figure 16-23: *a) & b) Image contrast enhancement by stretching. (a) Original image has poor contrast, due to clustering of DN's in histogram of pixel frequency versus DN count. (b) Stretching of DN values of pixels increases contrast in the image.*

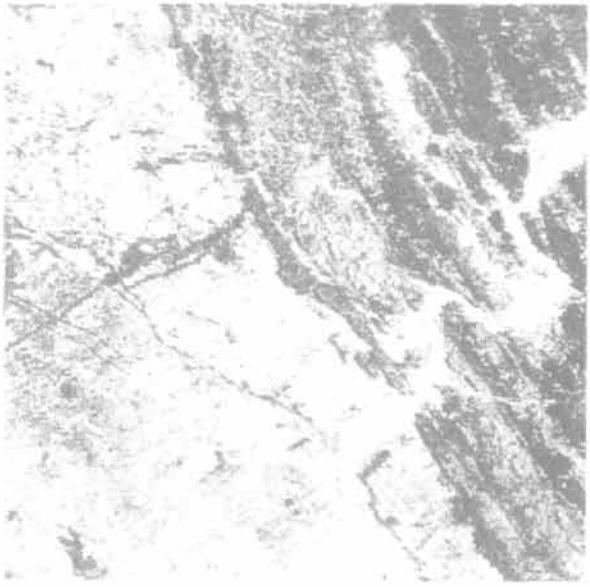

Figure 16-24a: *Landsat MSS image, using Band 7 only.*

Figure 16-24b: *Same Landsat MSS image of Figure 16-24a after ratioing of Bands 5 and 7.*

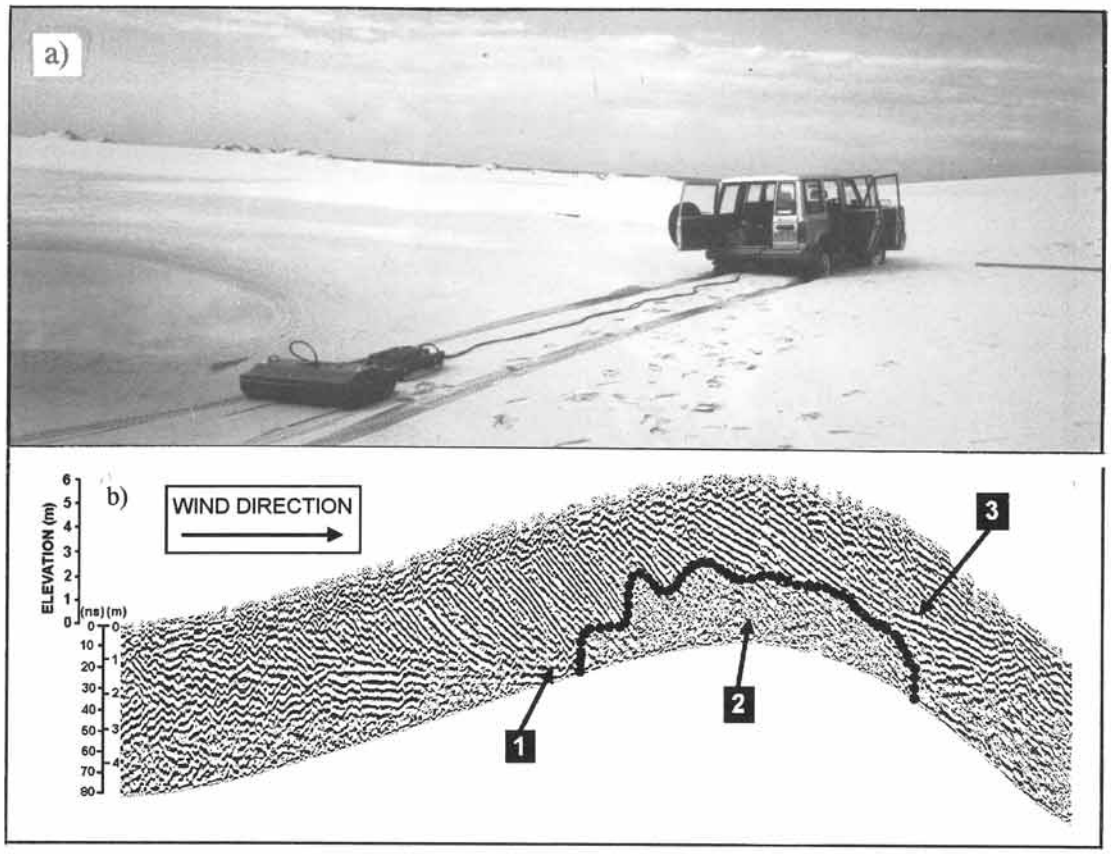

Figure 16-25: *a) & b) Ground Penetrating Radar system, towed behind a truck, can produce radargrams that resolve: (1) base of the dune, (2) zone of moisture, and (3) cross-stratification.*

☐Exercise 16-8: Convert the digital pixel print of Figure 16-22a into a color image by assigning colors to particular DN's.

16-8 Radar images

Radar (radio detection and ranging) has been traditionally used by military and civilian aviation authorities to monitor air space and ships at sea. It detects microwaves, which easily penetrate clouds, is insensitive to meteorological conditions, and is independent of daylight. The letter-coding of K, X, and L-bands (Fig. 16-1) originates from the Second World War, when it was used for security reasons.

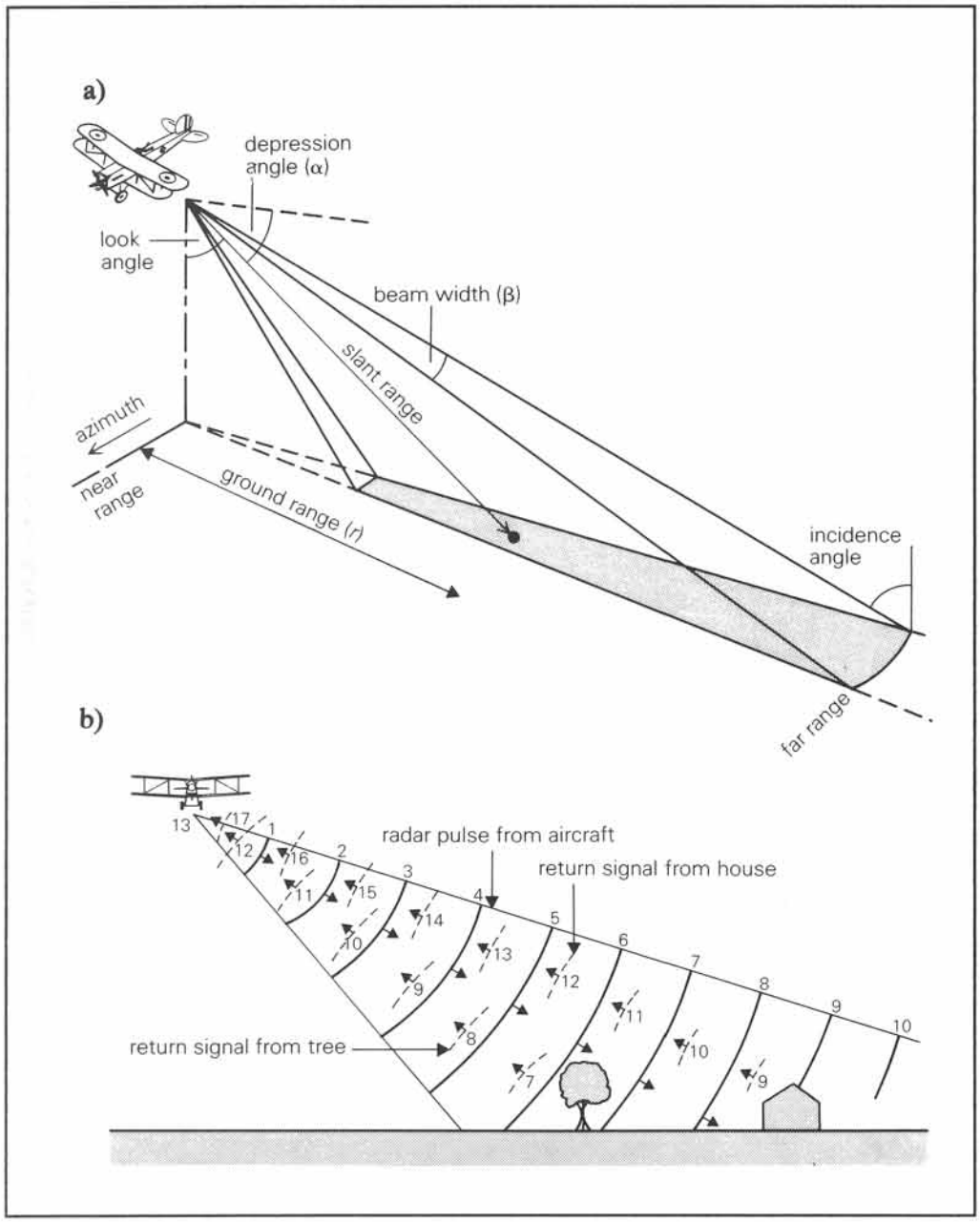

Figure 16-26: a) & b) Airborne radar is "side-looking" and distortions in the slant range increase with the incident angle of the pulsating radar signal.

In modern radar-imaging systems, microwave pulses generated by an antenna, are directed towards the ground surface. Radar wavefronts are backscattered and received by the same antenna before another pulse is emitted to the ground. The system can be carried in an aircraft, boat, or spacecraft. Ground Penetrating Radar (GPR) is a ground-based, remote sensing tool, used for non-destructive subsurface inves-

tigations. The antenna array is towed behind a truck and data are recorded in the field on a magnetic tape (Fig. 16-25a). The system differs from airborne radar in that the wave form is recorded in addition to the intensity. After processing the data in the office on a work station, the resulting image resembles a shallow seismic section, showing horizontal distance versus two-way travel time in vertical cross-sections (Fig. 16-25b). GPR can be used for mapping shallow geological structures down to twenty meters deep in dry sand.

Air and space-borne radar images typically have a sidelit character, resulting from cross-scanning of the surface while being overflown (Fig. 16-26a & b). Radar pulses can be transmitted in different modes of polarization, with vibrations restricted to a particular plane parallel to the direction of radar emission. Airborne radar images commonly have a fifty-kilometer-wide swath and resolution cells or pixels of ten to twelve meters width. Most commercial radar uses the K and X bands, which have negligible ground penetration. The backscattered electromagnetic

Figure 16-27a: *L-Band radar image, collected by Space Shuttle Endeavour from Wadi Sahba area, Saudi Arabia. The trace of the E-W trending Sahba fault is clearly visible. Image width is 40 kilometers.*

Figure 16-27b: *Landsat MSS image across same area portrayed in Figure 16-27a shows bedrock structures are entirely obscured by Ad Dhana sand sea. Thin E-W line in image is railway track.*

energy is controlled by the roughness and heterogeneity of the surface materials, their electrical properties (expressed in a dielectric constant), the slope of the ground surface, and the nature of the original microwave signal used to illuminate the ground surface.

Radar images have, also, been collected by NASA space shuttles carrying sophisticated radar systems. These include the L band, which may penetrate to six meters in depth into dry sand deposits. Moisture absorbs radarwaves, because the dielectric constant is greatly affected by the

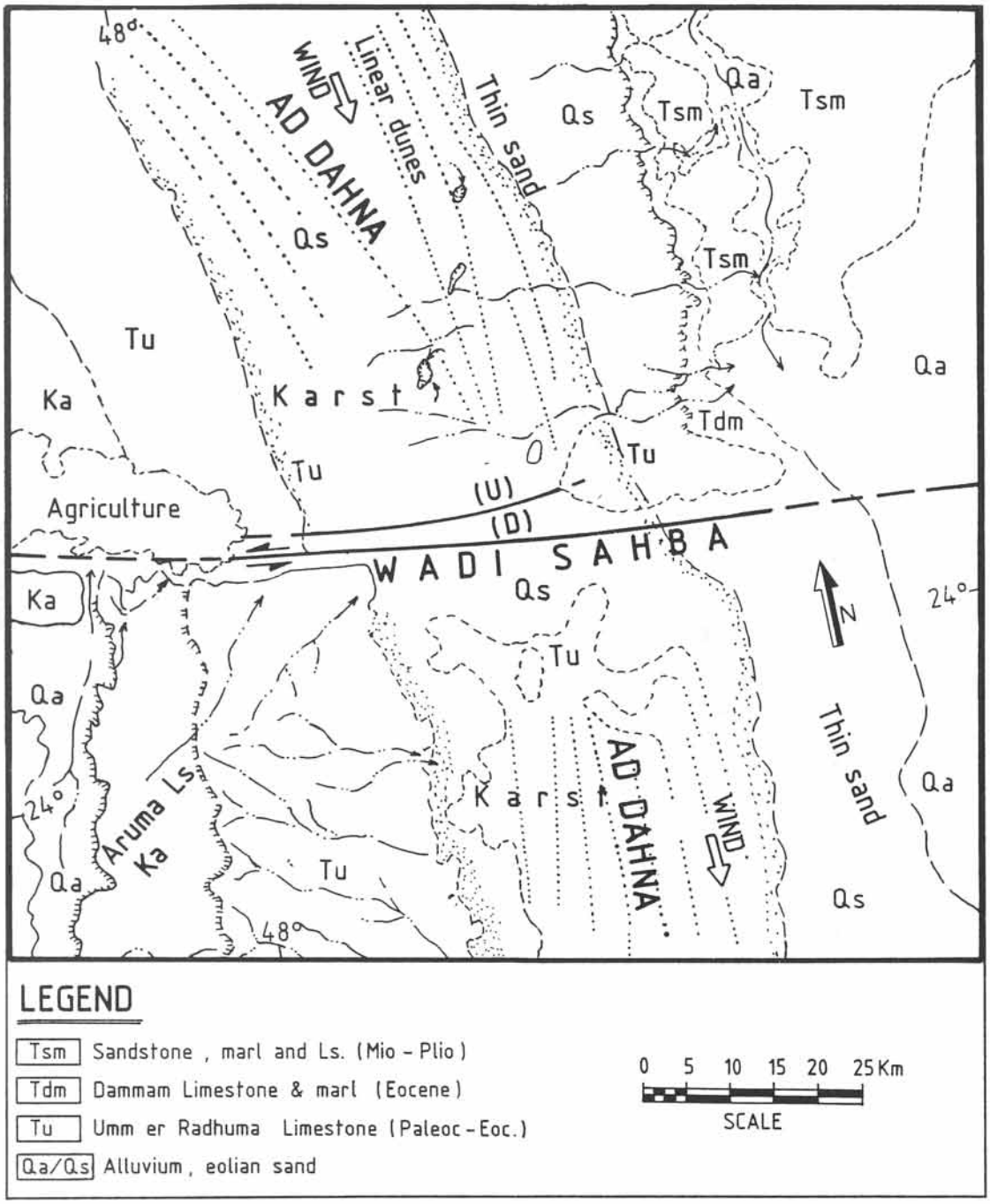

Figure 16-28: Geologic interpretation map of the Sahba fault, Saudi Arabia.

moisture content of the ground and, thus, reduces the penetration depth of radar methods.

Radar images using the L band may reveal shallow subsurface features, invisible on other remote sensing images. For example, the radar image of Figure 16-27a stretches across a section of Wadi Sahba, Saudi Arabia, where lower Tertiary strata are largely covered by the Ad Dhana sand sea. The drainage pattern and karst terrain incised in the bed rock below the Quaternary dune sand are clearly visible in the area north of Wadi Sahba, where the thickness of the sand sheet varies between two and ten meters. Such drainage patterns are relatively absent to the south along Wadi Sahba, where sand thickness exceeds ten meters and radar microwaves cannot reach the bedrock. The apparent change in bedrock depth on either side reflects a vertical component of relative movement. Topographic relief along the fault has been leveled by the drifting sand, which infills the low area on the south side of the fault. The Landsat image of Figure 16-27b confirms that the fault line is hidden beneath the eolian

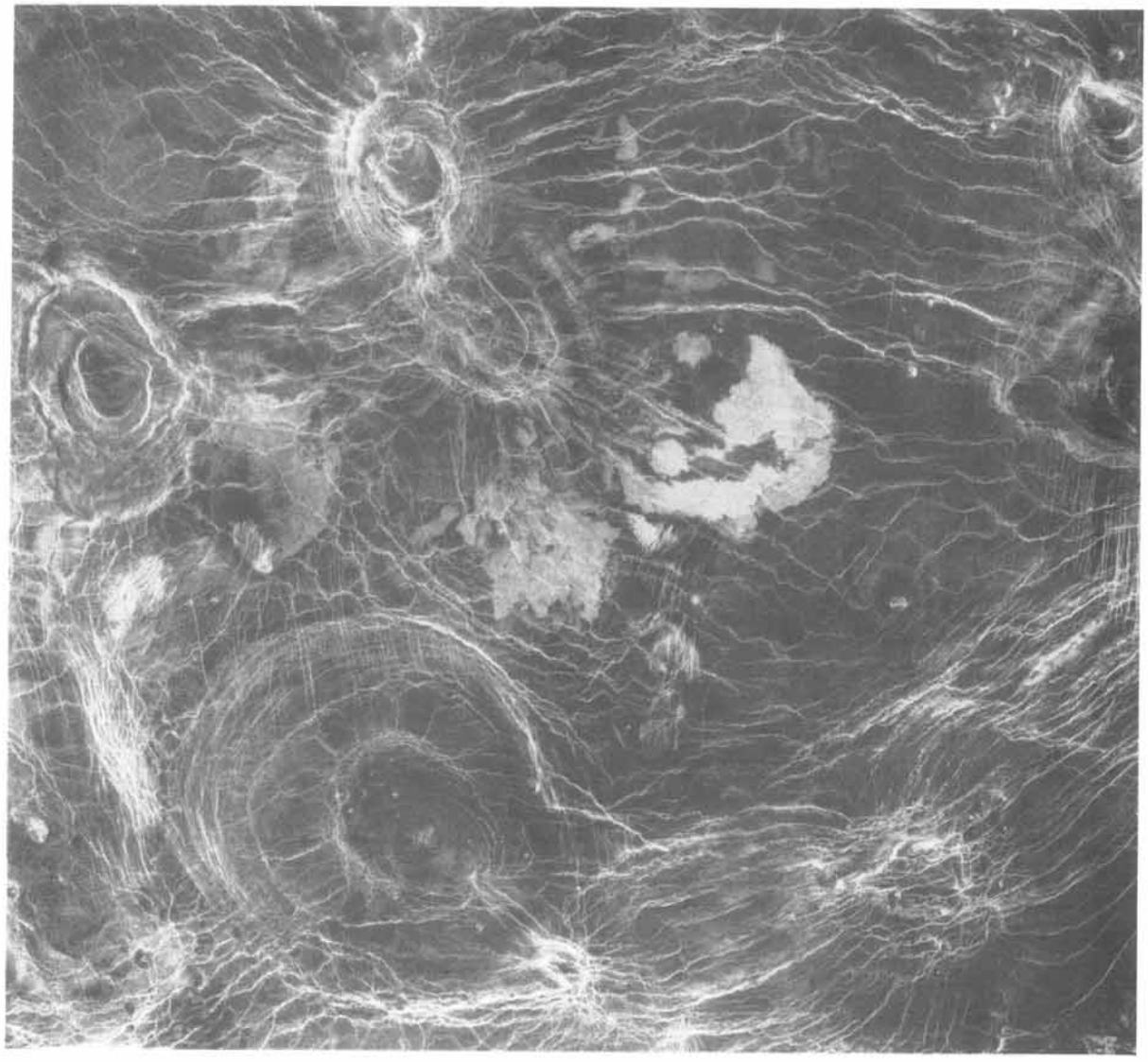

Figure 16-29: *Radar image collected by NASA's Magellan space probe from the surface of Venus. Shown are arachnoids with diameters ranging from 50 to 230 kilometers.*

sand and is revealed only by radar penetration along its northern side. The image interpretation map of Figure 16-28 indicates eight kilometers of apparent left-lateral displacement at the western end of the Wadi Sahba fault. This off-set is marked by exposed bedrock of Paleogene limestone.

Radar imaging has, also, been successfully used to explore the surface of various neighboring planets using a range of spacecraft missions. For example, Magellan is a NASA spacecraft launched in 1989 from aboard the Space Shuttle Atlantis. The spacecraft began its orbit around Venus in August 1990. A synthetic aperture radar (SAR) was used to penetrate the thick cloud cover, perpetually shielding the surface of Venus from vision. Figure 16-29 shows features, known as arachnoids, that have thus far been found on Venus only. They resemble spider and cobwebs and are circular to elliptical in shape with concentric rings and intricate outward-extending fractures. Arachnoids have diameters ranging from 50 to 230 kilometers. The bright lines, extending outward for many kilometers, may be dikes formed when magma upwelling from the planet's interior caused surface cracks. Arachnoids could be subvolcanic complexes with annular ring dikes and cone sheets, and radial igneous dikes. The bright patches in the center of the image are lava flows, indicating volcanic activity.

☐Exercise 16-9: Color the map of Figure 16-28 and compare this interpretation map with the original image of Figure 16-27a.